Optics Letters

Broadband dispersive Ge/YbF_3 mirrors for mid-infrared spectral range

Tatiana Amotchkina,[1,*] Michael Trubetskov,[2] Syed Ali Hussain,[1,2] Daniel Hahner,[1] Daniel Gerz,[1,2] Marinus Huber,[1,2] Wolfgang Schweinberger,[1,3] Ioachim Pupeza,[1] Ferenc Krausz,[1,2] and Vladimir Pervak[1]

[1]Ludwig-Maximilians-Universität München, Am Coulombwall 1, 85748 Garching, Germany
[2]Max-Planck-Institut für Quantenoptik, Hans-Kopfermann-Str. 1, 85748 Garching, Germany
[3]King Saud University, Department of Physics and Astronomy, Riyadh 11451, Saudi Arabia
*Corresponding author: Tatiana.Amotchkina@physik.uni-muenchen.de

Received 20 June 2019; revised 16 August 2019; accepted 8 September 2019; posted 13 September 2019 (Doc. ID 370564); published 18 October 2019

Broadband dispersive mirrors operating in the mid-infrared spectral range of 6.5–11.5 μm are developed for the first time, to the best of our knowledge. The mirrors comprise Ge and YbF_3 layers, which have not been used before for manufacturing of multilayer dispersive optics. The design and production processes are described; mechanical stresses of the coatings are estimated based on experimental data; and spectral and phase properties of the produced mirrors are measured. The mirrors compensate group delay dispersion of ultrashort laser pulses accumulated by propagation through 4 mm ZnSe windows and additional residual phase modulation of an ultrashort laser pulse. © 2019 Optical Society of America

https://doi.org/10.1364/OL.44.005210

In the course of recent developments of ultrafast laser technologies, multilayer optics is challenged by increasing demands on broadband dispersive mirrors (DMs) [1] exhibiting complicated spectral and phase properties as well as excellent adhesion, low mechanical stresses, and high laser damage thresholds. The current state of the art of dispersive optics can be found in the review [2] and references therein. Among a large variety of dispersive optical elements, DMs for the mid-infrared (MIR) spectral range are of great interest and novelty. MIR ultrashort pulses are used, for example, in highly sensitive MIR spectroscopy, gas spectroscopy, pump–probe experiments (see, e.g., [3–6]). DMs operating in the MIR spectral range are key optical elements to compensate for initial phase modulation of MIR pulses.

To the best our knowledge, Ref. [7] is until now the pioneering and only work reporting on MIR dispersive optics. The DM produced in Ref. [7] operates in the spectral range of 9–11.5 μm and exhibits average reflectance of 97.5% and group delay (GD) variation of 60 fs, which compensates for the GD accumulated by a pulse in a 1-mm-thick ZnSe window (see black curve in Fig. 1). The DM comprises layers of Ge and ZnS, contains 36 layers, and has a very large total thickness of 30.7 μm, resulting in an average absorption of 3%. Newly emerging broadband, temporally coherent MIR sources [8–15] set new demands on the bandwidth of dispersive optics.

In this Letter, for the first time, we report on the development of MIR DMs enabling with six bounces the compensation for GD with variation up to ∼400 fs over an almost octave-spanning spectral range of 6.5–11.5 μm (Fig. 1, red crosses). The sophisticated GD to be compensated for includes GD accumulated by a pulse in 4 mm ZnSe windows (green curve in Fig. 1) and additional phase modulation of the pulse. The GD behavior presented in Fig. 1 is quite typical for the MIR range, since in this range, almost all used substrates/windows (ZnSe, CaF_2, ZnS, KBr, YAG, BaF_2, sapphire, ZGP) delay the longer wavelengths with respect to the shorter wavelengths (see, e.g., GD accumulated in ZnSe windows shown in Fig. 1). For the sake of convenience of interested readers, in Fig. 1, we plot the GD accumulated in 1 mm ZnSe in 9–11.5 μm range in order to demonstrate that the present

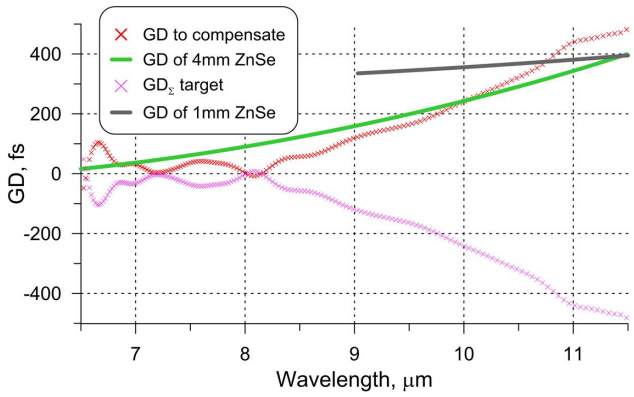

Fig. 1. GD to be compensated, GD accumulated in 4 mm ZnSe windows, and target GD_Σ to be achieved with the DM. GD accumulated in 1 mm ZnSe in 9–11.5 μm range is plotted as a reference.

DM problem is significantly more complicated than the one in [7] with GD variation of 60 fs.

In order to compensate for the GD shown in Fig. 1 by the red crosses, a very broadband, almost one-octave DM exhibiting high reflectance and complicated target $\hat{\mathrm{GD}}$ (Fig. 1, pink curve) had to be designed. The target $\hat{\mathrm{GD}}$ is nothing else but the GD to be compensated for taken with the opposite sign and shifted in vertical direction, since constant GD offset does not affect pulse shape. The choice of layer materials is a crucial issue. The widely known Ge/ZnS combination used for production of the DM operating in a much narrower range of 9–11.5 μm [7] does not permit a good approximation of the target characteristics in such a broad spectral region. A possible combination of ZnS and YbF_3 thin-film materials recently used for fabrication of a near-MIR beam splitter [16] provides even an lower refractive index ratio and is definitely not suitable for DM development.

The desired properties can be achieved by exploiting a thin-film combination with a large refractive index ratio. In the present work, Ge was chosen as a high-index material and YbF_3 as a low-index material; both materials are non-absorbing in the 6.5–11.5 μm range. The pair has been exploited for the first time for design and production of a complicated broadband beam splitter in our work [16]. In the operating spectral range, the ratio of the refractive indices of layer materials is 2.8. The refractive indices of Ge, YbF_3, and ZnSe substrate at 10 μm are 4.13, 1.47, and 2.43, respectively [16].

For designing the DM coating, needle optimization and gradual evolution algorithms of commercial OptiLayer software were used [17,18]. The layer thicknesses $d_1, \ldots, d_m$ were found based on the minimization of a merit function MF judging the approximation of target characteristics by actual spectral characteristics $R(d_1, \ldots, d_m; \lambda_j)$ and $\mathrm{GD}(d_1, \ldots, d_m; \lambda_j)$:

$$MF^2 = \sum_{j=1}^{161} \left[\frac{R(d_1, \ldots, d_m; \lambda_j) - \hat{R}(\lambda_j)}{\Delta_{j,R}}\right]^2 + \sum_{j=1}^{161} \left[\frac{\mathrm{GD}(d_1, \ldots, d_m; \lambda_j) - \hat{\mathrm{GD}}(\lambda_j)}{\Delta_{j,\mathrm{GD}}}\right]^2, \quad (1)$$

where $\{\lambda_j\}$ are evenly distributed wavelength points in the spectral range of 6.5–11.5 μm; $\hat{\mathrm{GD}}(\lambda_j)$ and $\hat{R}(\lambda_j) = 100\%$ are target GD and target reflectance values, respectively; m is the layer count, which is varied in the course of the design process; a small incidence angle of 5° and p polarization are assumed. In Eq. (1), $\Delta_{j,R}$ [%] and $\Delta_{j,\mathrm{GD}}$ [fs] are design tolerances.

The values shown in Fig. 1 by pink crosses are too broad and complicated to be achieved with the help of a single DM if we consider them as $\hat{\mathrm{GD}}(\lambda_j)$ target specifications in Eq. (1). Even if such a complicated GD could be theoretically synthesized, the production process would be very questionable. Inevitable presence of very thick layers could lead to cracking or peeling off the coating. In addition, large mechanical stresses in very thick layers could lead to thermal lensing that distorts the beam propagation in the entire laser system.

It is seen in Fig. 1 (pink crosses) that the target $\hat{\mathrm{GD}}$ variation of ~400 fs is too large to be compensated for by a single bounce. Designing the DM providing simultaneously high reflectance and large GD variation is not possible. A reasonable trade-off is to accumulate the required $\hat{\mathrm{GD}}$ using several bounces on identical DMs with a smaller GD variation. In this case, the total GD and total reflectance of N dispersive mirrors will be

$$\mathrm{GD}_\Sigma = N \cdot \mathrm{GD}, \qquad R_\Sigma = (R)^N. \quad (2)$$

Therefore, in Eq. (1), target $\hat{\mathrm{GD}}(\lambda_j)$ with N times smaller variation can be used: $\hat{\mathrm{GD}}(\lambda_j) = \mathrm{GD}_\Sigma(\lambda_j)/N$, while $\hat{R}(\lambda_j)$ target obviously remains the same.

For the design process, feasibility demands were taken into account. We tried to avoid large total thicknesses of the coating as well as large thicknesses of individual layers.

With $N = 2$, a good 24-layer DM solution with too large thickness of 15.5 μm containing 4.5 μm Ge and 11 μm YbF_3 was found. With $N = 4$, a quite thick 14-layer DM design of 12 μm thickness was synthesized. The design contained 3.8 μm Ge and 8.2 μm YbF_3; the thickness of one of the YbF_3 layers was 2.2 μm. The GD variations in these two cases were ~200 fs and ~100 fs, respectively.

A compromise was found for six bounces, i.e., $N = 6$. The corresponding target $\hat{\mathrm{GD}}$ is shown in Fig. 2 by blue crosses, and the GD variation is ~70 fs. As a result of the design process, a nine-layer solution with the refractive index profiles shown in Fig. 3 was obtained. The total physical thickness of the design was 6.4 μm, and total thicknesses of Ge and YbF_3 layers were 3.2 μm. The solution contained three YbF_3 and two Ge layers with thicknesses around 1 μm. For the sake of convenience, main parameters of the developed DMs and the DM from [7] are compared in Table 1.

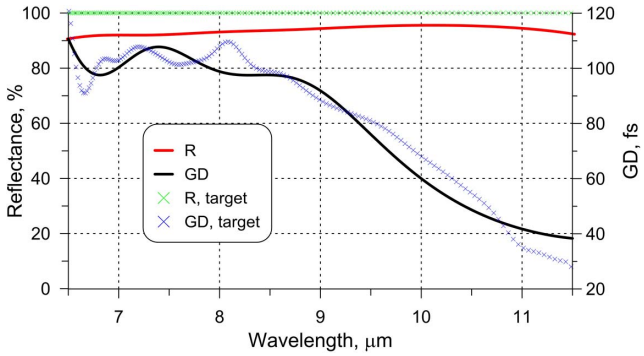

Fig. 2. Target and actual reflectance and GD of the nine-layer DM.

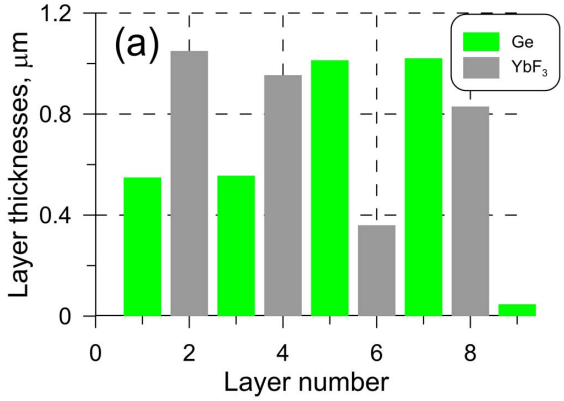

Fig. 3. Design structure of the DM.

Table 1. Comparison of the Present DM and DM from Ref. [7][a]

DM	N	Operating Range	Mat.	GD var., fs	R, %	Th., µm
Ref. [7]	1	9–11.5 µm (0.35 octave)	Ge/ZnS	60	97	30.7
This work	1	6.5–11.5 µm (0.82 octave)	Ge/YbF_3	67	95	6.4
	6			400	73.5	

[a]Mat. denotes thin-film materials, Th. is total physical thickness, var. is variation, N is the number of bounces.

Six DM samples were fabricated at the SyrusPro 710 high-vacuum system (Leybold Optics GmbH, Alzenau, Germany). The samples were based on the nine-layer DM design discussed above. The coatings were deposited on identical ZnSe substrates of 1 mm thickness. The vacuum system was pumped down to end vacuum 10^{-6} mbar before the process. The substrate temperature during the deposition was 120°C. The thin-film materials Ge and YbF_3 were initially in granules of 0.7–3.5 mm, purity 99.999%, and 1–3 mm, purity 99.99%, respectively. Before the process, the materials were molten in order to obtain solid blocks. The deposition rates for Ge and YbF_3 were 0.6 nm/sec and 0.3 nm/sec, respectively. Layer thicknesses were controlled using quartz crystal monitoring.

Several hours after opening the deposition plant, the adhesion of the coatings was tested with the help of a tape test, and the spectral characteristics of the coatings were measured. The tape test (kapton) proved the excellent adhesion of the coatings. Low stresses and good adhesion of the samples were achieved due to a properly developed deposition process for Ge/YbF_3. Stresses in separate layers of Ge and YbF_3 were reliably found with the help of Stoney formula [19,20] based on deflection values measured using the Dektak 150 Stylus Profiler (Veeco). These values are (–50 MPa) and 140 MPa for Ge and YbF_3, respectively. Stress of DM was calculated using the well-known approach from [20] and equaled 45 Mpa. Quasi-normal incidence reflectance data (Fig. 4) in the MIR range were recorded using a Fourier transform infrared spectrometer (Vertex 70, Bruker Optics GmbH).

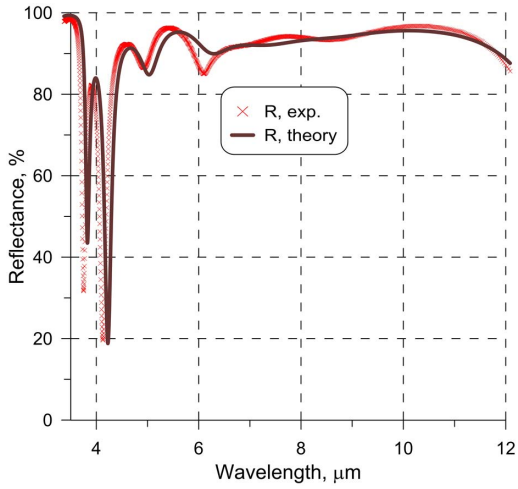

Fig. 4. Comparison of experimental and theoretical reflectance of the DM in the mid-infrared spectral range.

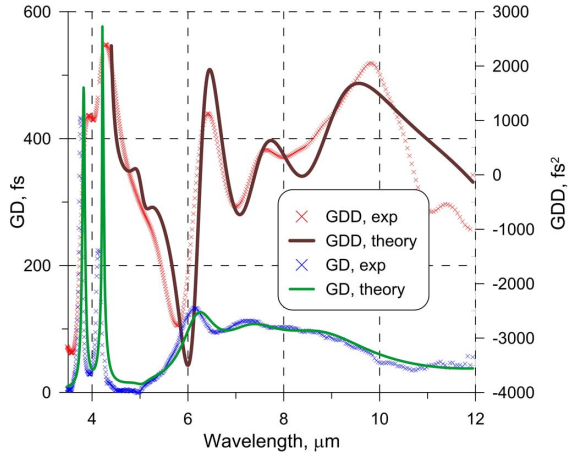

Fig. 5. Comparison of experimental and theoretical GD and GDD of the DM in the mid-infrared spectral range.

The GD experimental values of the DM were extracted from the data recorded by a MIR white-light interferometer developed in-house [21] (Fig. 5). The specific minima and maxima in the reflectance and GD curves were slightly shifted towards the shorter wavelengths compared to theoretical values. This suggests that the produced layers are thinner than expected. Still, the measured curves are in good agreement with the theoretical ones. Especially, the two very sharp peaks around 4 µm and the decline of about 100 fs from 6 µm to 12 µm in the GD curve could be measured. The reflectance also meets the theoretical curve across the whole requested range from 6.5 µm to 11.5 µm. Evidently, using six bounces, some part of pulse energy will be lost; this part is about 26.5% for 95% average reflectance of one mirror. For many applications, where the pulse duration/peak field is the decisive quantity, this decrease of average power is of secondary importance.

For experimental verification of the operation of our DMs, we tested them in a state-of-the-art broadband MIR field-resolving spectrometer. Few-cycle pulses spanning a –30 dB spectrum from 6.5 µm to 11.5 µm were generated via intrapulse difference-frequency mixing, and their electric field was detected via electro-optic sampling [8]. In the MIR beam path, we included a cuvette consisting of two ZnSe walls of 4 mm total thickness enclosing a layer of water. For several applications in field-resolved spectroscopy, the temporal compression of the excitation remaining after transmission through the sample is crucial. Figure 6 depicts the experimentally measured electric field of the initial chirped MIR pulse and the pulse

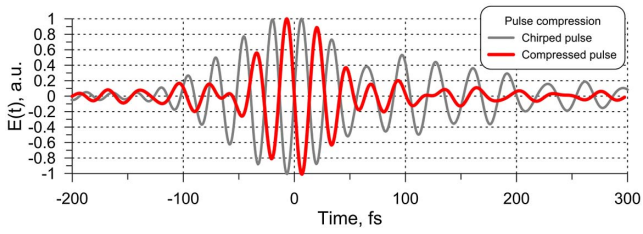

Fig. 6. Experimental normalized electric field in time domain: chirped pulse intensity FWHM duration is 86 fs, compressed pulse 55 fs.

compressed with six bounces off the new DM. The intensity full-width-half-maximum (FWHM) is reduced from 86 fs to 55 fs.

As the result, we demonstrated (1) high potential of Ge/YbF_3 thin-material combination for design and production of DMs and (2) unique DMs operating in the broadband MIR range.

Funding. Munich-Centre for Advanced Photonics.

REFERENCES

1. V. Pervak, O. Razskazovskaya, I. B. Angelov, K. L. Vodopyanov, and M. Trubetskov, Adv. Opt. Technol. **3**, 55 (2013).
2. A. Piegari and F. Flory, eds., *Optical Thin Films and Coatings: From Materials to Applications*, 2nd ed., Woodhead Publishing Series in Electronic and Optical Materials (Woodhead Publishing, Elsevier, 2018).
3. M. Huber, W. Schweinberger, M. Trubetskov, S. A. Hussain, O. Pronin, L. Vamos, E. Fill, A. Apolonski, M. Zigman, F. Krausz, and I. Pupeza, in *European Conference on Lasers and Electro-Optics and European Quantum Electronics Conference (CLEO/Europe-EQEC)*, Munich, Germany, 25 June 2017, paper CH-P_4.
4. A. Foltynowicz, P. Masłowski, A. J. Fleisher, B. J. Bjork, and J. Ye, Appl. Phys. B **110**, 163 (2013).
5. M. W. Todd, R. A. Provencal, T. G. Owano, B. A. Paldus, A. Kachanov, K. L. Vodopyanov, M. Hunter, S. L. Coy, J. I. Steinfeld, and J. T. Arnold, Appl. Phys. B **75**, 367 (2002).
6. A. V. Muraviev, V. O. Smolski, Z. E. Loparo, and K. L. Vodopyanov, Nat. Photonics **12**, 209 (2018).
7. F. Habel and V. Pervak, Appl. Opt. **56**, C71 (2017).
8. I. Pupeza, D. Sánchez, J. Zhang, N. Lilienfein, M. Seidel, N. Karpowicz, T. Paasch-Colberg, I. Znakovskaya, M. Pescher, W. Schweinberger, V. Pervak, E. Fill, O. Pronin, Z. Wei, F. Krausz, A. Apolonski, and J. Biegert, Nat. Photonics **9**, 721 (2015).
9. J. Zhang, K. Fai Mak, N. Nagl, M. Seidel, D. Bauer, D. Sutter, V. Pervak, F. Krausz, and O. Pronin, Light Sci. Appl. **7**, 17180 (2018).
10. C. Gaida, T. Heuermann, M. Gebhardt, E. Shestaev, T. P. Butler, D. Gerz, N. Lilienfein, P. Sulzer, M. Fischer, R. Holzwarth, A. Leitenstorfer, I. Pupeza, and J. Limpert, Opt. Lett. **43**, 5178 (2018).
11. M. Seidel, X. Xiao, S. A. Hussain, G. Arisholm, A. Hartung, K. T. Zawilski, P. G. Schunemann, F. Habel, M. Trubetskov, V. Pervak, O. Pronin, and F. Krausz, Sci. Adv. **4**, eaaq1526 (2018).
12. T. P. Butler, D. Gerz, C. Hofer, J. Xu, C. Gaida, T. Heuermann, M. Gebhardt, L. Vamos, W. Schweinberger, J. A. Gessner, T. Siefke, M. Heusinger, U. Zeitner, A. Apolonski, N. Karpowicz, J. Limpert, F. Krausz, and I. Pupeza, Opt. Lett. **44**, 1730 (2019).
13. Q. Wang, J. Zhang, A. Kessel, N. Nagl, V. Pervak, O. Pronin, and K. F. Mak, Opt. Lett. **44**, 2566 (2019).
14. S. Vasilyev, I. S. Moskalev, V. O. Smolski, J. M. Peppers, M. Mirov, A. V. Muraviev, K. Zawilski, P. G. Schunemann, S. B. Mirov, K. L. Vodopyanov, and V. P. Gapontsev, Optica **6**, 111 (2019).
15. C. Gaida, M. Gebhardt, T. Heuermann, F. Stutzki, C. Jauregui, J. Antonio-Lopez, A. Schülzgen, R. Amezcua-Correa, A. Tünnermann, I. Pupeza, and J. Limpert, Light Sci. Appl. **7**, 94 (2018).
16. T. Amotchkina, M. Trubetskov, M. Schulz, and V. Pervak, Opt. Express **27**, 5557 (2019).
17. A. V. Tikhonravov, M. K. Trubetskov, and G. W. DeBell, Appl. Opt. **35**, 5493 (1996).
18. A. V. Tikhonravov and M. K. Trubetskov, "OptiLayer software," http://www.optilayer.com.
19. A. E. Ennos, Appl. Opt. **5**, 51 (1966).
20. K. Hendrix, J. D. T. Kruschwitz, and J. Keck, Appl. Opt. **53**, A360 (2014).
21. F. Habel, M. Trubetskov, and V. Pervak, Opt. Express **24**, 16705 (2016).

130.183.92.9 {ts '2019-11-27 05:01:33'}